

**SYNTHESIS, MODIFICATION AND
IMMOBILIZATION OF
COPPER BENZENE-1,3,5-TRICARBOXYLATE
FOR THE REMOVAL OF METHYLENE BLUE
IN WASTEWATER**

SIEW WEI YUAN

UNIVERSITI SAINS MALAYSIA

2020

**SYNTHESIS, MODIFICATION AND
IMMOBILIZATION OF
COPPER BENZENE-1,3,5-TRICARBOXYLATE
FOR THE REMOVAL OF METHYLENE BLUE
IN WASTEWATER**

by

SIEW WEI YUAN

**Thesis submitted in fulfilment of the requirements
for the degree of
Master of Science**

July 2020

ACKNOWLEDGEMENT

I would like to express my deepest gratitude and appreciation to my supervisor Assoc. Prof. Dr. Noor Hana Hanif Abu Bakar for her guidance, knowledge, motivation and financial support throughout the journey of my postgraduate studies. Her supportive motivation and suggestions while introducing this beautiful field of Metal Organic Framework has been one of the most impactful changes in my life. Thanks for providing lots of opportunity for me to attend conferences, colloquiums and the Sakura Japan Exchange Programme. These have definitely widen my perspective about scientific research and have been some of the greatest moment in my life.

I would also like to thank Professor Mohamad Abu Bakar, for his much-valued guidance in crystallography and other scientific discussions during my research. Thanks for reviewing all my publications and giving lots of beneficial comments for me to improve my writing. His postgraduate experience has always inspires and excited me to start a new study on my own.

Special thanks to the School of Chemical Sciences for providing all the required instruments to complete my research project. I would also like to extend my sincere gratitude to all the science officers and technical staff for their various contribution directly or indirectly in analysing all my samples throughout this project.

I would also like to thank my seniors in Assoc. Prof. Dr. Noor Hana Hanif Abu Bakar`s group, especially Asmaa, Najwa, Nana, Liza, Fatin, and Dr. Nazrina for helping me through the research project. Thank you for spending time explaining theories to me while still being friendly to me all time.

My sincere thanks for Sam Suat Peng for her utmost help, support and wise suggestions in handling all my obstacles and difficulties and special care that I have

received every single day during this chapter for my life. Thanks for accompanying me since bachelor degree, and giving me encouragement during difficult times.

I would also like to thank Universiti Sains Malaysia for awarding me the USM fellowship that funds my master study and keep my busy all time.

Last but not least, thanks to my family for supporting me in pursuing my dream in doing scientific research. Thank you so much for the encouragement and spiritual support during all time.

Siew Wei Yuan

July 2020

TABLE OF CONTENTS

ACKNOWLEDGEMENT	ii
TABLE OF CONTENTS	iv
LIST OF TABLES	viii
LIST OF FIGURES	x
LIST OF ABBREVIATIONS, SYMBOLS & UNITS	xiv
ABSTRAK	xvii
ABSTRACT	xix
CHAPTER 1 INTRODUCTION	1
1.1 Brief Overview	1
1.2 Problem Statements.....	2
1.3 Objectives of Study	3
1.4 Scope of Study	3
1.5 Thesis Layout	4
CHAPTER 2 LITERATURE REVIEW	5
2.1 Metal organic framework (MOF).....	5
2.2 Design of metal organic framework.....	6
2.2.1 Inorganic connector.....	6
2.2.2 Linker	7
2.2.3 Secondary building unit (SBU).....	9
2.3 Synthesis of MOF.....	10
2.4 Common MOF	11
2.4.1 Copper benzene-1,3,5-tricarboxylate (CuBTC).....	12
2.4.2 Iron benzene-1,3,5-tricarboxylate (FeBTC).....	13
2.5 Bimetallic organic framework.....	14
2.6 Application of MOF	15

2.6.1	Gas storage and separation.....	15
2.6.2	Catalytic reaction	16
2.6.3	Liquid phase adsorption	17
2.6.4	Methylene blue dye adsorption	18
2.7	Polymer	21
2.7.1	Synthetic polymer	21
2.7.2	Natural polymer	22
	2.7.2(a) Polyhydroxyalkanoates (PHA).....	23
2.8	Immobilization of MOF	24
2.8.1	Mixed-matrix membrane.....	24
2.8.2	Free-standing MOF membrane	25
2.9	Characterization techniques	26
2.9.1	Field emission scanning electron microscopy	27
2.9.2	N ₂ adsorption-desorption analysis	28
2.9.3	X-Ray Diffraction (XRD)	32
2.9.4	Fourier-transform Infrared Spectroscopy (FTIR)	33
2.9.5	Thermogravimetric Analysis (TGA).....	34
CHAPTER 3 METHODOLOGY		36
3.1	Materials.....	36
3.2	Synthesis of MOF.....	36
3.2.1	Synthesis of Copper Benzene-1,3,5-tricarboxylate, [Cu ₃ (BTC) ₂ (H ₂ O) ₃] _n	36
3.2.2	Synthesis of Iron Benzene-1,3,5-tricarboxylate (FeBTC)	37
3.2.3	Synthesis of Bimetallic Benzene-1,3,5-tricarboxylate.....	37
3.3	Polyhydroxybutyrate (PHB).....	38
3.3.1	Purification of PHB.....	38
3.3.2	Hydrolytic degradation of PHB	39
3.3.3	PHB film casting.....	39

3.3.4	Film casting for PHB-supported CuBTC.....	39
3.4	Characterization techniques	40
3.5	Determination of pH zero point of charge (pH _{pzc})	41
3.6	Kinetics adsorption of MB	42
3.6.1	Reusability study.....	42
3.7	Isotherm study	43
3.8	Statistical study	43
CHAPTER 4 THE INFLUENCE OF GREEN SYNTHESIS ON THE FORMATION OF VARIOUS COPPER BENZENE-1,3,5- TRICARBOXYLATE COMPOUNDS		44
4.1	Introduction	44
4.2	Determination of CuBTC Phase via FTIR and XRD Analysis.....	46
4.3	Surface Properties and Morphology.....	52
4.4	Thermal Properties	56
4.5	Adsorption of MB by Cu-BTC.....	58
4.6	Kinetics for the adsorption of MB on CuBTC	60
4.7	Summary	69
CHAPTER 5 POLYHYDROXYBUTYRATE AND COPPER BENZENE- 1,3,5-TRICARBOXYLATE COMPOSITE FILMS FOR THE ADSORPTION OF METHYLENE BLUE DYE.....		70
5.1	Introduction	70
5.2	Characterization	72
5.2.1	PHB-CuBTC composite.....	72
5.2.2	PHB-PVP-CuBTC composite	80
5.3	Adsorption Studies	82
5.3.1	Effect of Amount of PHB in the PHB-CuBTC Composite	82
5.3.2	Effect of Different Molecular Weight of PHB.....	84
5.4	The presence of Polyvinylpyrrolidone (PVP) in the film	86
5.5	Kinetics for the adsorption of MB.....	90

5.6	Adsorption isotherm of MB	95
5.7	Reusability.....	99
5.8	Summary	100
CHAPTER 6 INFLUENCE OF VARIOUS Cu/Fe RATIOS ON THE SURFACE PROPERTIES OF Cu-Fe-BTC AND IT'S RELATION TO METHYLENE BLUE ADSORPTION		101
6.1	Introduction	101
6.2	Determination of compound via FTIR,XRD and AAS analysis.....	102
6.3	Surface properties and morphology	106
6.4	Thermal properties	112
6.5	Adsorption of dye by MOF samples	114
6.6	Kinetics for the adsorption of dye by MOF samples	116
6.7	Adsorption isotherms	122
6.8	Summary	127
CHAPTER 7 CONCLUSION AND FUTURE RECOMMENDATIONS		128
7.1	Conclusion.....	128
7.2	Recommendations for Future Research	130
REFERENCES.....		131
APPENDICES		
LIST OF PUBLICATIONS		

LIST OF TABLES

	Page
Table 2.1	Adsorption capacity of modified and un-modified CuBTC.....20
Table 3.1	Synthesis method for the preparation of CuBTC.....37
Table 3.2	The weight of $\text{FeCl}_2 \cdot 4\text{H}_2\text{O}$ and $\text{Cu}(\text{OAC})_2 \cdot \text{H}_2\text{O}$ for the synthesis of bimetallic metal organic framework samples.38
Table 4.1	BET surface area of CuBTC samples.54
Table 4.2	Pseudo first-order and pseudo-second order kinetics models.....61
Table 4.3	Pseudo first-order and pseudo second-order rate constant by linear method for sorption of MB into different CuBTC catalyst.....63
Table 4.4	Pseudo first-order and pseudo second-order rate constant by non-linear method for sorption of MB into different CuBTC catalyst.....67
Table 5.1	BET surface area of CuBTC , PHB-CuBTC and PHB-PVP-CuBTC76
Table 5.2	Surface roughness of all films via AFM82
Table 5.3	Gel permeation chromatography (GPC) results for PHB and hydrolysed PHB.85
Table 5.4	Pseudo first-order and pseudo second-order rate constant by non-linear method for sorption of MB into CuBTC, PHB-CuBTC and PHB-PVP-CuBTC.92
Table 5.5	The rate of adsorption analysed under intraparticle diffusion by CuBTC and the composites.....95
Table 5.6	Langmuir and Freundlich isotherm parameters for MB adsorption.98
Table 6.1	Elementary analysis via atomic adsorption spectroscopy for metal organic framework compounds.....105

Table 6.2	BET surface area and pH_{pzc} for metal organic framework compounds.	106
Table 6.3	MB adsorption capacity of metal organic framework compounds. .	115
Table 6.4	Pseudo first-order and pseudo second-order rate constant by non-linear method for sorption of MB into metal organic framework compounds.	119
Table 6.5	The intra-particle diffusion constant and linear regression coefficient for different metal organic framework.	121
Table 6.6	Langmuir and Freundlich isotherm parameters for MB adsorption.	125

LIST OF FIGURES

	Page
Figure 2.1	Molecular structure of benzene-1,4-dicarboxylate (BDC) and benzene-1,3,5-tricarboxylate(BTC)5
Figure 2.2	Common shapes for a molecule with a different number of coordination sites.7
Figure 2.3	Example of linker used in the construction of MOF.....8
Figure 2.4	Assembly of the metal organic framework, coordination of metal ion to organic linker to form secondary building unit (SBU) and linked secondary building will form an expanded framework or solid. Metal (purple), oxygen (red) and carbon (gray).....9
Figure 2.5	The molecular structure of CuBTC where copper, oxygen, carbon and hydrogen are labeled in blue, red, grey and white colour respectively.13
Figure 2.6	Structural motifs of Cu-Ru-BTC, (left) Cu-Ru paddle wheel; (right) Cu-Cu paddlewheel.....15
Figure 2.7	Chemical structure of MB.....19
Figure 2.8	Chemical structure of polymers.22
Figure 2.9	Chemical structure of linear polysaccharides such as cellulose, chitin and chitosan.23
Figure 2.10	Molecular structure of polyhydroxybutyrate.24
Figure 2.11	Combination of MOF and polymer component to produce mixed-matrix membrane.25
Figure 2.12	Electrospun nanofibrous skeleton for the fabrication of free-standing MOF membranes.26
Figure 2.13	Diagram of the ET detector [102].28
Figure 2.14	IUPAC classification of N ₂ isotherm [104].29

Figure 2.15	Classification of hysteresis loop [104].....	31
Figure 2.16	Illustration setup of an ATR element with liquid sample.	34
Figure 4.1	The molecular structure of (a) $[\text{Cu}_3(\text{BTC})_2(\text{H}_2\text{O})_3]_n \cdot 10_n \text{H}_2\text{O}$ (1) and (b) $[\text{Cu}_2(\text{OH})(\text{BTC})(\text{H}_2\text{O})]_n \cdot 2_n \text{H}_2\text{O}$ (2) where copper, oxygen, carbon and hydrogen are labeled in blue, red, grey and white colour respectively. The graphic was simulated using Mercury software version 4.0.0 (Cambridge Crystallographic Data Centre) and CIF from Chui <i>et al.</i> [12] and Chen <i>et al.</i> [52].....	45
Figure 4.2	IR spectra for CuBTC samples.	48
Figure 4.3	IR spectrum for sample C (activate at 120°C) and sample C (activated at 180°C).....	49
Figure 4.4	PXRD pattern of CuBTC samples and reference structure of $\text{Cu}_2(\text{OH})(\text{BTC})(\text{H}_2\text{O}) \cdot 2\text{H}_2\text{O}$ (2) from Chen <i>et al.</i> , [52] and $\text{Cu}_3(\text{BTC})_2(\text{H}_2\text{O})_3 \cdot 10\text{H}_2\text{O}$ (1) from Chui <i>et al.</i> , [12].....	51
Figure 4.5	N_2 -adsorption desorption isotherm plot and pore size distribution of CuBTC samples	53
Figure 4.6	Scanning electron microscope images of samples with (i) magnification of 8000 × and (ii) magnification of 30000 ×.....	55
Figure 4.7	Profile of (a) DTG of CuBTC samples; (b) TGA of CuBTC samples.....	57
Figure 4.8	The graph of (a) q_t (mg dye/ g adsorbent) against time (min); (b) Adsorption capacity, q_e (mg dye/ g adsorbent) against BET surface area (m^2/g).....	59
Figure 4.9	(a) Pseudo second-order by type 1 linear method for adsorption of CuBTC samples; (b) Pseudo first-order by non-linear method for adsorption of CuBTC samples; (c) Pseudo second-order by non-linear method for adsorption of CuBTC samples	65
Figure 5.1	IR spectra for PHB ,CuBTC, PVP, PHB-CuBTC, PHB-PVP and PHB-PVP-CuBTC.	73

Figure 5.2	X-ray diffraction spectrum of PHB , CuBTC, PHB-CuBTC, PHB-PVP, and PHB-PVP-CuBTC. The major peaks in PHB and CuBTC were denoted as A and B, respectively.	74
Figure 5.3	N ₂ adsorption-desorption of CuBTC and the composites.	76
Figure 5.4	Scanning electron microscopy images of (A) PHB, (B) CuBTC, (C) PHB-CuBTC , (D) PHB-PVP and (E) PHB-PVP-CuBTC. (i) magnification of 8000 × and (ii) magnification of 30000 ×.	78
Figure 5.5	AFM images of (a) PHB, (b) PHB-CuBTC, (c) PHB-PVP and (d) PHB-PVP-CuBTC	79
Figure 5.6	The effect of different amount of PHB with 10 mg of CuBTC towards the adsorption capacity of MB and time required to reach adsorption equilibrium. Mean data accompanied by different alphabet letters are significantly different (Tukey test, $p < 0.05$).	84
Figure 5.7	The effect of different molecular weight of 100 mg PHB with 10 mg of CuBTC towards the adsorption capacity of MB and time required to reach adsorption equilibrium. Mean data accompanied by different alphabet letters are significantly different (Tukey test, $p < 0.05$).	86
Figure 5.8	Potential zero charge of PHB, CuBTC, PHB-CuBTC , PHB-PVP and PHB-PVP-CuBTC samples.	88
Figure 5.9	The equilibrium time and adsorption capacity of MB for CuBTC and its composites.	89
Figure 5.10	Kinetic modelling of CuBTC, PHB-CuBTC, PHB-PVP-CuBTC via 1 st order kinetic and 2 nd order kinetic model.	91
Figure 5.11	Kinetic adsorption of CuBTC and CuBTC composites analysed under intraparticle diffusion model.	95
Figure 5.12	Nonlinear Langmuir and Freundlich adsorption isotherm plot for (a) CuBTC and (b) PHB-CuBTC , (c) PHB-PVP-CuBTC	97
Figure 5.13	Reusability of CuBTC and CuBTC composite.	100
Figure 6.1	FTIR spectra of different metal organic framework compound.	103

Figure 6.2	Powder X-ray diffraction pattern different metal organic framework compound.	104
Figure 6.3	N ₂ sorption isotherm plot and pore size distribution different Fe/Cu weight ratio metal organic framework samples.	108
Figure 6.4	Pore width distribution of each compounds via non-local density functional theory (NLDFT) slit type pore.	109
Figure 6.5	Scanning electron microscopy images of sample A (CuBTC), B (Cu ₉₃ Fe ₇ BTC), C (Cu ₈₂ Fe ₁₈ BTC), D (Cu ₆₇ Fe ₃₃ BTC), E (Cu ₅₃ Fe ₄₇ BTC) and F (FeBTC) with (i) 8000× and (ii) 30000× magnification	110
Figure 6.6	The profile of (a) Thermogravimetric analysis data and (b) differential thermal analysis data for MOF compounds.	113
Figure 6.7	The kinetics data of metal organic framework compounds plot with q _t (mg dye/g adsorbent) against Time (min) in pseudo-first-order and pseudo-second-order non-linear model.	117
Figure 6.8	Intraparticle diffusion plot for metal organic framework compounds.	122
Figure 6.9	Nonlinear Langmuir and Freundlich adsorption isotherm plot for (a) CuBTC, (b) Cu ₉₃ Fe ₇ BTC, (c) Cu ₈₂ Fe ₁₈ BTC, (d) Cu ₆₇ Fe ₃₃ BTC, (e) Cu ₅₃ Fe ₄₇ BTC and (f) FeBTC.....	126

LIST OF ABBREVIATIONS, SYMBOLS & UNITS

Å	Angstrom
AAS	Atomic Absorption Spectroscopy
ABS	Acrylonitrile Butadiene Styrene
AFM	Atomic Force Microscopy
BBC	4,4',4''-(benzene-1,3,5-triyl-tris(benzene-4,1-diyl))tribenzoic acid
BDC	Benzene-1,4-benzenedicarboxylate
BDPC	biphenyl-4,4'-dicarboxylate
BET	Brunauer-Emmett-Teller
BTB	1,3,5-benzenetribenzoate
BTC	Benzene-1,3,5-tricarboxylate
BTE	4,4',4''-[benzene-1,3,5-triyl-tris(ethyne-2,1-diyl)]tribenzoate
cm ⁻¹	per centimeter
CTAB	Cetyltrimethylammonium Bromide
Cu ²⁺	Copper Ion
CuBTC	Copper Benzene-1,3,5-tricarboxylate
Cu _x Fe _x BTC	Copper-Iron Benzene-1,3,5-tricarboxylate
Đ	polydispersity index
DMF	Dimethylformamide
DTG	Differential Thermogravimetric
ET	Everhart-Thornley
EtOH	Ethanol
Fe ²⁺	Iron Ion
FeBTC	Iron Benzene-1,3,5-tricarboxylate
FESEM	Field Emission Scanning Electron Microscope
FTIR	Fourier-Transform Infrared Spectroscopy

g	Gram
GO	Graphite Oxide
H ₃ BTC	Trimesic acid
HCl	Hydrochloride Acid
K	Kelvin
M	Molarity
mg	Milligram
mL	Milliliter
MMM	Mixed-matrix membrane
MOF	Metal Organic Framework
NaOH	Sodium Hydroxide
nm	Nanometer
NMR	Nuclear Magnetic Resonance
°C	Degree Celcius
PHA	Polyhydroxyalkanoates
PHB	Polyhydroxybutyrate
pH _{pzc}	pH point of zero charge
ppm	Parts per million
PVP	Polyvinylpyrrolidone
PXRD	Powder X-Ray Diffraction
q _e	Adsorption Capacity
s	Second
SBU	Secondary Building Unit
SCXRD	Single-Crystal X-Ray Diffraction
SEM	Scanning Electron Microscope
STP	Standard Condition of Temperature and Pressure
TG	Thermogravimetric

TGA Thermogravimetric Analysis
XRD X-Ray Diffraction

**SINTESIS, MODIFIKASI DAN IMMOBILISASI
KUPRUM BENZENA-1,3,5-TRIKARBOKSILAT UNTUK PENJERAPAN
METILINEA BIRU DALAM AIR KUMBAHAN**

ABSTRAK

Kaedah sintesis hijau telah digunakan untuk mensintesis $[\text{Cu}_3(\text{BTC})_2(\text{H}_2\text{O})_3]_n$ (CuBTC). Kaedah yang ditubuhkan hanya menggunakan air sebagai pelarut sintesis dan ia boleh dilakukan pada suhu bilik. Dalam sistem sintesis yang sama, sebatian kedua, $\text{Cu}_2(\text{OH})(\text{BTC})(\text{H}_2\text{O}) \cdot 2\text{H}_2\text{O}$ telah berjaya disintesis dengan perubahan prosedur sintesis. Sebatian ini digunakan untuk menjerapan pewarna metilena biru (MB). CuBTC menunjukkan keupayaan penjerapan yang lebih tinggi berbanding $\text{Cu}_2(\text{OH})(\text{BTC})(\text{H}_2\text{O}) \cdot 2\text{H}_2\text{O}$. Hal ini berlaku kerana CuBTC mempunyai luas permukaan BET dan isipadu liang yang lebih tinggi. Dua cara yang berbeza telah diguna untuk meningkatkan prestasi penjerapan. Antaranya ialah penyediaan komposit polihidroksibutirat-CuBTC (PHB-CuBTC) dan pengubahan pusat logam CuBTC dengan menambahkan sejumlah besi ke pusat logam untuk menghasilkan rangka organik dwilogam (BMOF). Semua sampel telah dicirikan menggunakan analisis penjerapan penyerapan N_2 , mikroskop pengimbasan elektron dan spektroskopi inframerah jelmaan Fourier (FTIR). Kewujudan PHB menggalakkan penjerapan MB. Komposit PHB-CuBTC (24.49 mg/g) telah menunjukkan kapasiti penjerapan yang lebih tinggi berbanding CuBTC (16.03 mg/g). Penambahan polivinilpirolidon (PVP) kepada komposit PHB-CuBTC membolehkan penjerapan metil oren (MO) dan mengurangkan masa yang diperlukan untuk mencapai keseimbangan bagi penjerapan MB. Seterusnya, suatu siri Cu-Fe-BTC telah berjaya disintesis. Luas permukaan BET

bagi Cu₈₂Fe₁₈BTC (1240 m²/g) jauh lebih tinggi daripada CuBTC (708 m²/g). Peningkatan selanjutnya dalam peratus Fe₂₊ akan mengurangkan luas permukaan sebatian. Kewujudan Fe₂₊ dalam rangka sebatian telah berjaya mengganggu pembentukan liang dan meluaskan saiz liang pada permukaan sebatian BMOF. Selain itu, pH_{pzc} yang berkaitan dengan keasidan permukaan memainkan peranan penting dalam proses penjerapan. Berbanding CuBTC, Cu₅₃Fe₄₇BTC dengan kapasiti penjerapan sebanyak 94.42 mg/g telah menunjukkan 6 kali lebih kapasiti penjerapan terhadap MB. Ini telah menunjukkan bahawa dengan menggunakan nisbah tembaga dan logam kedua yang berbeza, mungkin boleh merangka morfologi permukaan BMOF secara berkesan untuk aplikasi tertentu.

**SYNTHESIS, MODIFICATION AND IMMOBILIZATION OF
COPPER BENZENE-1,3,5-TRICARBOXYLATE FOR THE REMOVAL OF
METHYLENE BLUE IN WASTEWATER**

ABSTRACT

A series of green synthesis methods were applied to synthesize $[\text{Cu}_3(\text{BTC})_2(\text{H}_2\text{O})_3]_n$ (CuBTC). The established method uses only water as the synthesis solvent and it is able to be carried out at room temperature. By applying the same synthesis system, a second compound, $\text{Cu}_2(\text{OH})(\text{BTC})(\text{H}_2\text{O}) \cdot 2\text{H}_2\text{O}$ was successfully synthesized by altering the synthesis procedure. These compounds were subjected to the removal of methylene blue (MB) dye. CuBTC shows greater adsorption capability compared to $\text{Cu}_2(\text{OH})(\text{BTC})(\text{H}_2\text{O}) \cdot 2\text{H}_2\text{O}$ as CuBTC exhibits higher BET surface area and pore volume. Two different approaches were used to further enhance the performance of the adsorbent which are the preparation of polyhydroxybutyrate-CuBTC (PHB-CuBTC) composite and altering the metal center of CuBTC by adding different amounts of iron into the metal center to produce bimetallic organic frameworks (BMOFs). All samples were subjected to N_2 adsorption-desorption analysis, scanning electron microscope (SEM), and Fourier transform infrared spectroscopy (FTIR). Presence of PHB promotes the adsorption of MB, thus PHB-CuBTC composites (24.49 mg/g) shows greater adsorption capacity when compared to CuBTC (16.03 mg/g). The addition of polyvinylpyrrolidone (PVP) into PHB-CuBTC allows small amount of methyl orange (MO) adsorption and reduced the time required to achieve adsorption equilibrium for MB adsorption as compared to PHB-CuBTC. Subsequently, a series of Cu-Fe-BTC were successfully synthesized. The BET surface area of $\text{Cu}_{82}\text{Fe}_{18}\text{BTC}$ (1240 m^2/g) was significantly higher than

CuBTC (708 m²/g). Further increase in the Fe²⁺ percentage will reduce the surface area of the compound. The presence of Fe²⁺ in the framework successfully disturbs the pore formation and widens the pore size on the surface of BMOFs compounds. This as well as the p*H*_{pzc}, which is related to the surface acidity of the resulting BMOF, play an important role in the adsorption process. Cu₅₃Fe₄₇BTC with an adsorption capacity of 94.42 mg/g shows approximately 6 times greater adsorption capacity against MB compared to CuBTC. This shows that by utilizing a different ratio of Cu and a second metal, it is possible to effectively design the surface morphology of BMOF for specific applications.

CHAPTER 1

INTRODUCTION

1.1 Brief Overview

The use of porous material as adsorbent and catalyst has increased since the great industrial revolution. Currently, two of the most commonly used porous materials in the world are zeolite and activated carbon [1], [2]. Both of these materials have different characteristics as zeolite is highly crystalline with interconnected pores of 4 – 13 Å, while activated carbon is a highly porous amorphous material [2], [3]. The microporous lattice of zeolite systems is useful in size-selective catalysis or grouping of small organic molecules, albeit it is still not favourable for many applications. Zeolite materials are predominantly made up from boron, aluminium, gallium, silicon, phosphorus and bridged by oxygen [2]. The incorporation of transition metal into the compound will often lead to a collapsed framework. In contrast, the disordered porous structure of activated carbon is formed from the twisted network of defective hexagonal carbon layers and cross-linked by aliphatic bridging groups [4]. A crystalline material with tuneable pore size is highly desirable for applications. Therefore, the limitations faced by zeolite and activated carbon have motivated many scientists to look for a compound that forms a porous framework and has properties that are beyond zeolite compound [5], [6]. Recently, a new class of compound namely metal organic framework (MOF) has drawn researchers' attention. The idea of these new compounds was first been reported by Yaghi *et al.* [7]. He demonstrated that the design of an open and rigid framework is possible to be achieved via molecular chemistry and the resulting compound was able to have great thermal and crystal lattice stability even after losing the guest molecules [7]. The syntheses of MOFs are carried out at mild condition and the selection of metal and organic linker can lead to

the desired extended network [4]. Besides that, this material shows lots of attractive features such as high surface area, tunable uniform pore size, and excellent chemical solvent stability which can be utilised under many applications [8].

1.2 Problem Statements

The interest of utilising MOF for commercial purposes has increased. Various MOF's have been synthesized to produce optimized compounds for specific application. However, the cost of the synthesis has become a major obstacle to apply MOF in the field. Usage of organic solvents and heat required for solvothermal synthesis has resulted in relatively high costs. Besides that, the ability of designing and altering the pore size of MOF's or MOF polymer composite is also very important to enhance the performance for adsorption of organic contaminant in water to regenerating clean water. A new synthesis method that only utilises water as the only solvent during synthesis at room temperature can greatly help to reduce the cost of synthesis. However, this has yet to be established. Furthermore, to date, most the polymer-MOF composites have been focused on the use of synthetic polymers. The study of a biopolymer-MOF composite for adsorption application is few. Besides that, the characterisation and performance of bimetallic organic frameworks (BMOFs) for the adsorption of MB are not understood in depth.

1.3 Objectives of Study

The objectives of this study are:

1. To synthesize and characterize CuBTC prepared at room temperature with only the use of H₂O as the solvent.
2. To investigate the adsorption capacity of CuBTC against MB dye.
3. To determine the effect of CuBTC immobilized onto PHB and PHB-PVP film against MB dye adsorption.
4. To synthesize and characterize BMOFs (Cu-Fe-BTC) and to investigate its effectiveness towards the removal of MB dye via adsorption.

1.4 Scope of Study

This study has been limited to the synthesis of CuBTC with the use of H₂O as the only solvent. Different synthesis procedures were applied to investigate the best synthesis route for CuBTC. In order to enhance the adsorption capacity of CuBTC, CuBTC was immobilized onto a PHB and a mixture of PHB/PVP thin film. Besides that, different ratio of copper : iron precursor solution was introduced during syntheses to form BMOFs, Cu-Fe-BTC. The characterization techniques that were applied to investigate the synthesized products were thermogravimetric analysis (TGA), N₂ adsorption-desorption, Fourier-transform infrared spectroscopy (FTIR), X-ray powder diffraction (XRD), atomic absorption spectroscopy (AAS), scanning electron microscopy (SEM) as well as atomic force microscopy (AFM). The samples were then used in adsorption of MB dye.

1.5 Thesis Layout

This thesis consists of seven chapters. The first chapter is the introduction of this study which highlights the problem statements, objectives and scope of study. Chapter two is literature review which will cover the fundamental knowledge related to the subject of this thesis. The experimental procedure and materials of this project is discussed in chapter three. In chapter four, results on the synthesis and characterization of CuBTC via different techniques are presented. The adsorption properties of these MOF's are also discussed. Chapter five shows the results of immobilizing CuBTC with PHB or PHB/PVP to form a mix-matrix membrane for MB adsorption. Chapter six is the modification of CuBTC with Fe to form CuFeBTC and enhance the adsorption performance of the adsorbent. Lastly, chapter seven concludes this research project and provides recommendations for future work in this field.

CHAPTER 2

LITERATURE REVIEW

2.1 Metal organic framework (MOF)

In 1990, Robson and Hoskins [9] proposed a new class of crystalline compounds specifically MOF which can be obtained through self-assembly of metal ions and multifunctional organic ligands. The covalent bonding of polydentate ligands to the metal center is the basic foundation of MOF. Therefore, the amount of energy required to overcome the activation energy is low, thus the reaction can be carried in relatively mild conditions. This also opens up the possibility of designing specific framework geometry via different ligands and metal combination.

The research on MOF was ignited after Yaghi *et al.* [10] reported an interesting compound which was obtained by copolymerization of 1,4-benzenedicarboxylate (BDC) with Zn_{2+} ions which acted as the secondary building unit (SBU) of MOF-5 in extending a three-dimensional framework. The compound maintained its structural integrity even as the guest species were removed from the framework, thus providing a robust open framework structure that has a huge permanent porosity of estimated 2900 m^2/g (Langmuir surface area) [11].

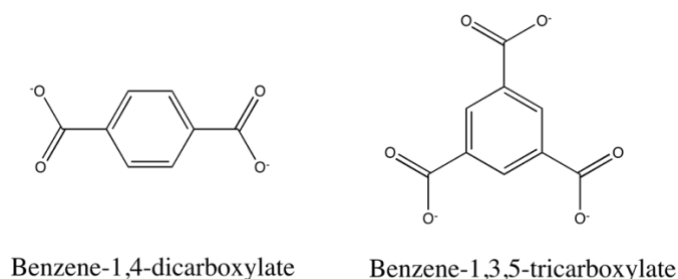


Figure 2.1 Molecular structure of benzene-1,4-dicarboxylate (BDC) and benzene-1,3,5-tricarboxylate(BTC)

2.2 Design of metal organic framework

Formation of MOF is mainly constructed by two starting reagents which are the inorganic connector and organic linker. Via a different combination of these two key components, MOF can be designed to have different optical, electrical, magnetic, catalytic and structural properties.

2.2.1 Inorganic connector

Transition metals are often used as the inorganic connector as they have different oxidation states and coordination numbers which give different molecular geometries (Figure 2.2) [4], [12]. D-block elements can have coordination numbers ranging from 2 to 7 which give rise to linear, T-shaped, square planar, square-based pyramidal and octahedral geometries. Unusual topologies are formed by using lanthanide which has large coordination numbers from 7 to 10 [4]. Removal of coordinated solvent molecules from the lanthanide ion center can generate coordinatively unsaturated metal center which can be utilised for adsorption and catalysis applications. Therefore, the final geometry of the compound depends on the numbers of functional sites that bond with the organic linker.

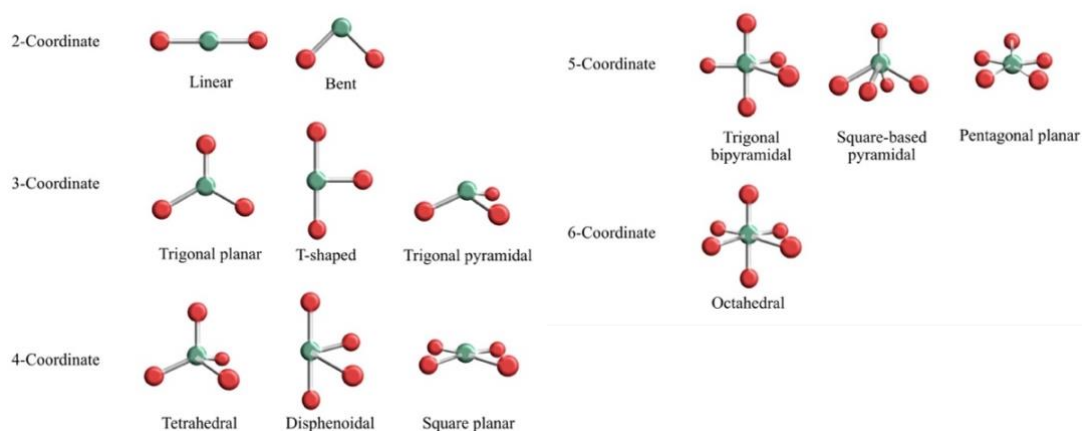


Figure 2.2 Common shapes for a molecule with a different number of coordination sites.

2.2.2 Linker

Generally, linkers can be divided into four specific groups which are inorganic, neutral organic, anionic organic and cationic organic ligand (Figure 2.3) [4]. The simplest and smallest linker is halides while CN-, SCN- and cyanometallate have similar bridging ability as halides which coexist with neutral organic ligands in MOF structures. Pyrazine and bipyridine are the most frequently used neutral organic ligand in the construction of MOF [4], [13]–[15]. Carboxylate are the typical anionic organic linker in the coordination framework [4]. Cationic ligand are less employed in MOF as their low affinity for cationic metal ions does not favour in forming a stable framework. All bridging ligands should be rigid as they are required to maintain the structural integrity of the compound even after the removal of guest molecules in the pores [16]. Therefore, organic linkers containing benzene rings are widely used in the structure. Increasing the hydrocarbon chain can form an elongated linker, typical example are 1,2-bis(4-pyridyl) ethane and bipyridine. The use of elongated linker in coordination can effectively increase the void spaces in the structure, but they are weaker to support the framework compared to short organic linker [17]–[19]. Therefore, the framework is much more easily collapsed after the removal of guest molecules [17]–[19].

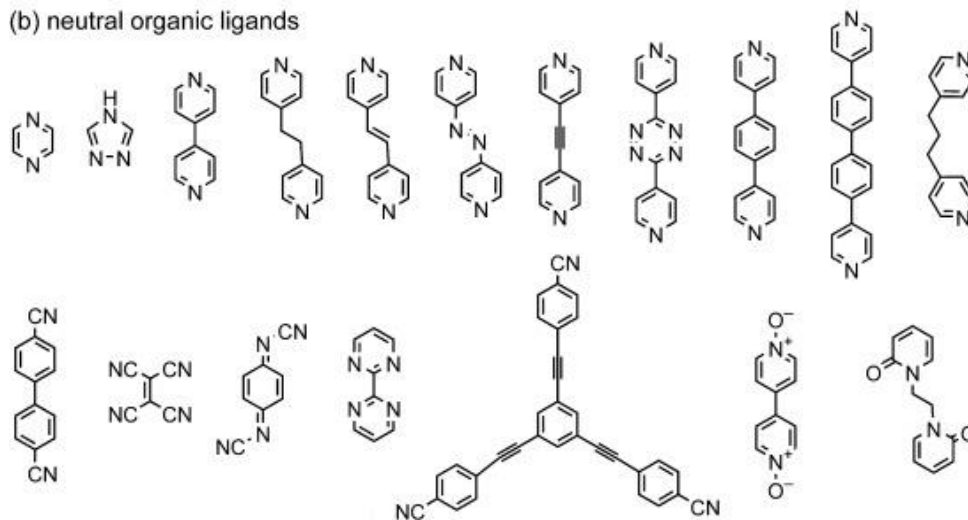
(a) inorganic ligands

Halides (F, Cl, Br, and I)

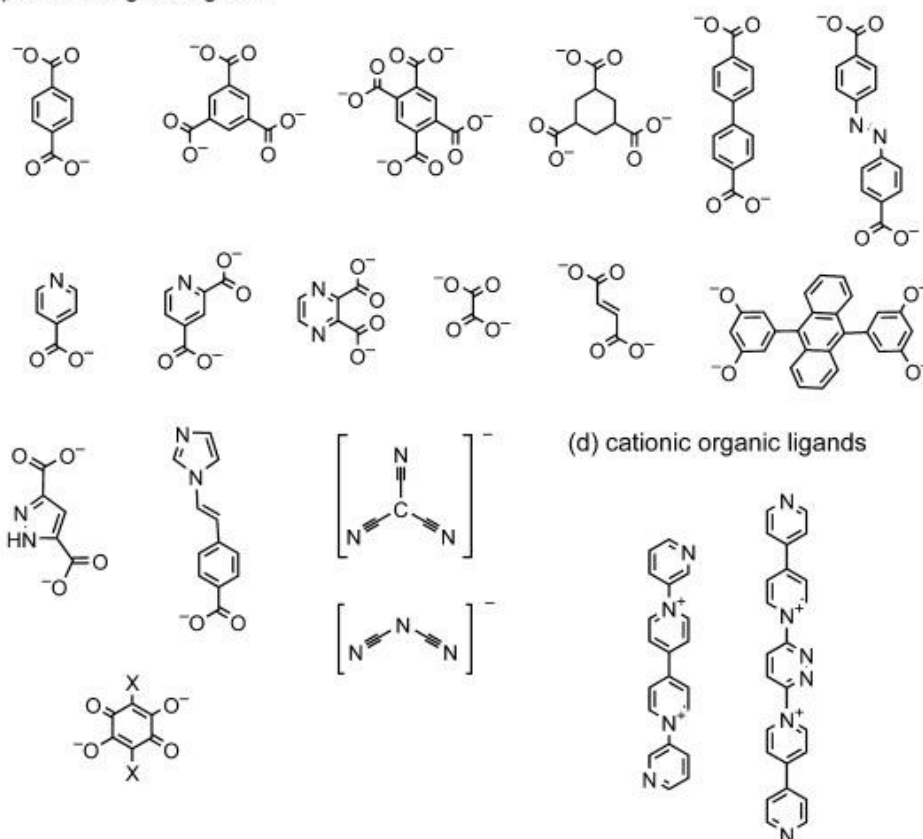
Cyanometallate ($[M(CN)_x]^{n-}$)

CN^- SCN^-

(b) neutral organic ligands



(c) anionic organic ligands



(d) cationic organic ligands

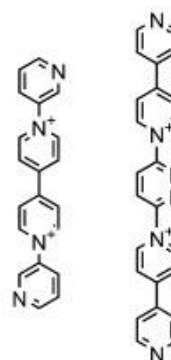


Figure 2.3 Example of linker used in the construction of MOF.

2.2.3 Secondary building unit (SBU)

Coordination of multidentate carboxylate linkers to two or more metal ions will form a polynuclear cluster called secondary building unit (SBU). SBUs will then be linked and assembled into a three dimensional solid (Figure 2.4) [18]. Figure 2.4 shows that 1,4-benzenedicarboxylate (BDC) first forms a rigid cluster with metal ions. The rigid cluster namely SBU has 6-connecting vertices which has an octahedral geometry can subsequently form an extended cube framework as cube by combining with other SBUs. The geometry of the MOF can be predicted and comprehended by the special coordination number and geometry of SBU. As the carboxylate groups in the organic linker lock down the position of metal ions, SBU has sufficient rigidity to produce an extended framework with high structural stability. The constructed neutral framework avoids the need for counterions in the cavities. Removal of auxiliary ligands will free the coordination site which enables the reactive metal sites to be studied [4]. MOFs maintain their structural integrity even after removal of these auxiliary ligands and the empty ligand sites form pores that can be utilised for other applications [11].

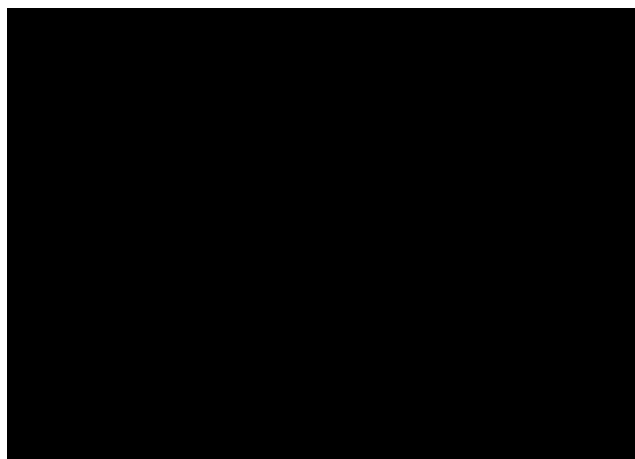


Figure 2.4 Assembly of the metal organic framework, coordination of metal ion to organic linker to form secondary building unit (SBU) and linked secondary building will form an expanded framework or solid. Metal (purple), oxygen (red) and carbon (gray).

2.3 Synthesis of MOF

One of the most common synthesis methods for MOF is via solvothermal synthesis. Conventionally, small scale solvothermal synthesis involves electrically heating precursor solutions in a small vial or sealed NMR tube while large batch synthesis is carried out in a Teflon-lined stainless steel autoclave [20]. However, this method usually requires maintaining the system at a high temperature for long periods of time. Therefore, scientists have attempted to prepare MOF through microwave-assisted [21], sonochemical [22], electrochemical [23] and mechanochemical [21] methods to lower down the required time, energy and simplify the synthesis procedure.

Microwave-assisted technique usually involves microwave equipment that applies an oscillating electric field to the synthesis medium. The electric field which is coupled with the permanent dipole moment of the molecules then induces molecular rotation and results in homogenous rapid heating of the solution [21]. Therefore, crystallization of nanoporous material can occur in a shorter time with less energy required compared to the solvothermal system. Features such as adjustable power output, fibre optic temperature and pressure controller are normally included in the microwave equipment [24]. The synthesis procedure involves placing a substrate mixture with a suitable solvent in a sealed Teflon vessel and placing it into the microwave unit. It has been reported that higher phase purity, higher yield and better reproducibility of MOF's can be obtained with the practice of microwave-assisted solvothermal method [21], [25].

The sonochemical technique is a method that utilizes ultrasonic waves to initiate the synthesis reaction. As sonication is performed to the substrate solution, the formation and collapse of bubbles formed in the solution will produce high local temperature (~5000 K) and pressure (~1000 bar) [26]. This results in extremely fast

heating and cooling rates, which can produce fine crystallites. Armstrong *et al.* [22] have reported the synthesis of CuBTC in DMF/water solvent via sonochemical technique. The reaction time required was reduced from 12 h for solvothermal synthesis to 30 min when using this synthesis technique.

Others synthesis procedure such as room temperature synthesis is highly desirable to reduce the amount of energy required [27][28]. A synthesis procedure that avoids the need of organic solvents during synthesis can also reduce the cost of MOF production [20].

2.4 Common MOF

$Zn_4O(4,4',4''\text{-[benzene-1,3,5-triyl-tris(ethyne-2,1-diyl)]tribenzoate})(\text{biphenyl-4,4'-dicarboxylate})$ [$Zn_4O(\text{BTE})(\text{BPDC})$], $Zn_4O(4,4',4''\text{-[benzene-1,3,5-triyl-tris(benzene-4,1-diyl)]tribenzoate})_2$ [$Zn_4O(\text{BBC})_2$], $Zn_4O(1,3,5\text{-benzenetribenzoate})_2$ [$Zn_4O(\text{BTB})_2$], $Zn_4O(1,4\text{-benzenedicarboxylate})_3$ [$Zn_4O(\text{BDC})_3$], and $Cu_3(\text{BTC})_2(\text{H}_2\text{O})_3$ and $Fe\text{BTC}$ are some of the most studied compounds as they possess interesting characteristics. Among these compounds, $Zn_4O(\text{BTE})(\text{BPDC})$, $Zn_4O(\text{BBC})_2$, $Zn_4O(\text{BTB})_2$, $Zn_4O(\text{BDC})_3$, were reported by Fukukawa *et al* [29]. These compounds were utilizing the octahedral $Zn_4O(\text{CO}_2)_6$ as their unit in the building the MOF structures. $Zn_4O(\text{BTE})(\text{BPDC})$ has one of the highest BET surface area (6240 m^2/g) among MOF compounds [29]. $Zn_4O(\text{BBC})_2$ has also one of the highest Langmuir surface area of 10400 m^2/g which is capable to store 2860 mg/g of CO_2 . $Cu_3(\text{BTC})_2(\text{H}_2\text{O})_3$ is well known for its pore stability, while $Fe\text{BTC}$ was known as a solid acid which is great for catalytic reaction [30], [31].

2.4.1 Copper benzene-1,3,5-tricarboxylate (CuBTC)

Copper(III) benzene-1,3,5-tricarboxylate $[\text{Cu}_3(\text{BTC})_2(\text{H}_2\text{O})_3]_n$ (**1**) is synthesized by copper salt and benzene-1,3,5-tricarboxylic acid (H_3BTC). This porous metal coordinate polymer was first reported by Chui *et al.*, in 1999 and it is currently one of the most investigated MOF in literature and associated with more than 2900 scientific articles based on Google Scholar [12], [32]. In general, CuBTC (Figure 2.5) [12] has a three-dimensional system of channels and accessible porosity. The high surface area, uniform pore size, accessible coordinate unsaturated sites, and excellent chemical solvent stability make CuBTC a great candidate for catalyst and sorbent in liquid phase [8]. It is commonly named as HKUST-1 or CuBTC and has received greater attention after the discovery of its good stability against moisture and excellent thermal stability compared to MOF-5 [24].

In most metal-ligand systems, a wide range of possible compound can be found [12], [33], [34]. Besides $[\text{Cu}_3(\text{BTC})_2(\text{H}_2\text{O})_3]_n$ (**1**), one of the most commonly found compound in the copper and benzene-1,3,5-tricarboxylate (BTC) system is $[\text{Cu}_2(\text{OH})(\text{BTC})(\text{H}_2\text{O})]_n$ (**2**). Therefore, extensive works have been conducted to investigate how different conditions such as the type of metal salt [21], [35], solvent [21], [35], pH [36], temperature [21] and synthesis method [37] can yield the target compound and influence the properties of the final $[\text{Cu}_3(\text{BTC})_2(\text{H}_2\text{O})_3]_n$ (**1**). Furthermore, literature has shown that the surface area of $[\text{Cu}_3(\text{BTC})_2(\text{H}_2\text{O})_3]_n$ (**1**) can vary between 331 and 1944 m^2/g depending on the synthesis conditions however the reproducibility of these highly porous materials has been questioned [12], [38], [39].

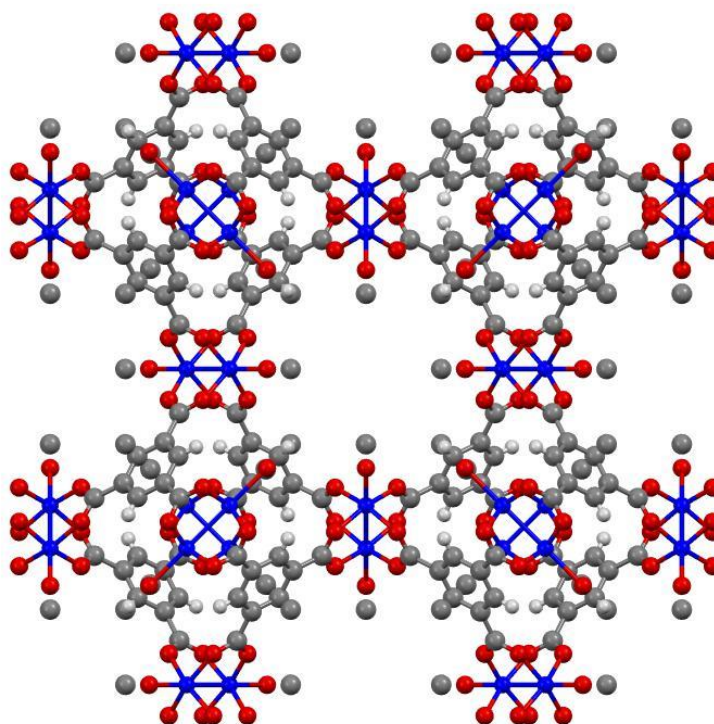


Figure 2.5 The molecular structure of CuBTC where copper, oxygen, carbon and hydrogen are labeled in blue, red, grey and white colour respectively.

2.4.2 Iron benzene-1,3,5-tricarboxylate (FeBTC)

Iron 1,3,5-benzenetricarboxylic (FeBTC) is synthesized from iron salt and H₃BTC. It is also known as Basolite F300 and was reported to be effective in removing Azo-dye orange II compounds from aqueous solutions via adsorption [40]. The adsorption capacities of FeBTC were reported to be much higher when compared to activated carbon [40]. Besides that, the removal of arsenic from aqueous solution using FeBTC showed that it has more than 6 times greater adsorption capacities compared to iron oxide nanoparticles of 50 nm [41]. Despite great adsorption properties, FeBTC display amorphous characteristics when examined under X-ray powder diffraction, thus the crystal lattice of FeBTC is yet to be confirmed [30].

2.5 Bimetallic organic framework

Since the discovery of MOF's, scientists are trying to enhance the characteristic and performance of the compound for desired application such as catalysis and adsorption [42], [43]. One of the interesting attempts is to introduce a second metal element into the framework during synthesis or post-synthesis, thus a BMOF is yielded (Figure 2.6) [42], [44]. Figure 2.6 demonstrate a paddlewheel structure of a bimetallic framework in CuBTC [45]. Ge *et al.* [44] demonstrated that BMOF Mn/Co-BTC exhibits high catalytic performance for oxidative coupling of benzylamines while Hu *et al.* [46] proved that incorporating a small amount of Ni into CuBTC framework enhanced the capacity and performance for adsorption of anionic dye. Selection of the second metal element is based on the higher affinity of the element for desired applications [43]. However, several reports illustrated that the BET surface area dropped as the second metal ion is incorporated into CuBTC framework [44], [46]. Metals with different ionic sizes in the framework will cause coordination defect and disturb the formation of crystal structure, thus preventing the full formation of 3D porosity [45], [47], [48]. The incorporation of two metal elements in the framework might induce defects which might enhance or weaken the desired characteristic. Therefore the selection of base framework and the incorporated second metal must be carefully examined. Nevertheless, incorporation of two different metal ions in the framework has increased the possibility of designing a suitable adsorbent with desired surface morphology.

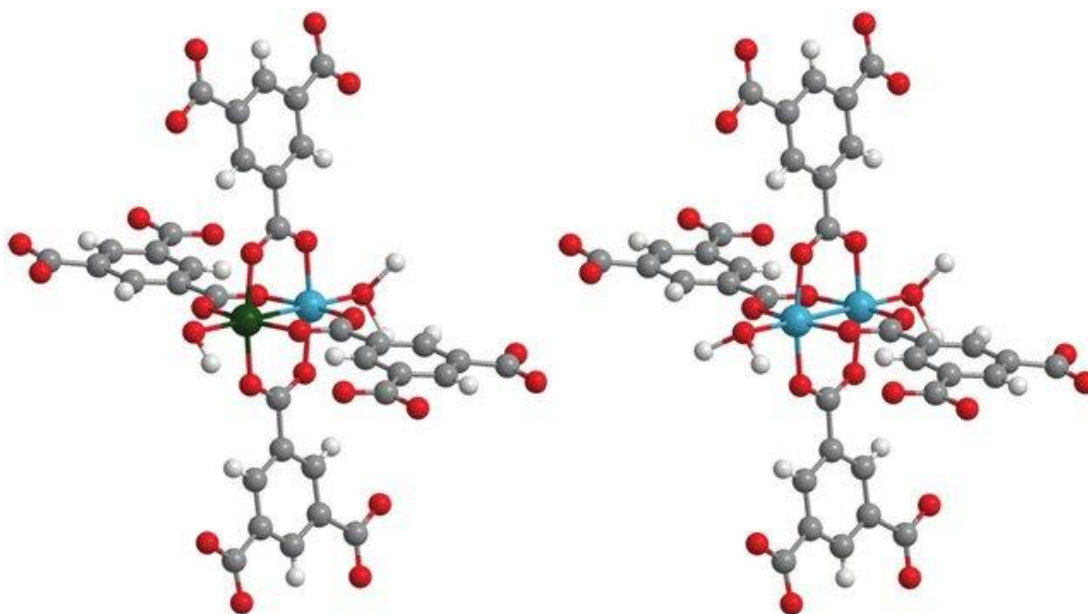


Figure 2.6 Structural motifs of Cu-Ru-BTC, (left) Cu-Ru paddle wheel; (right) Cu-Cu paddlewheel.

2.6 Application of MOF

2.6.1 Gas storage and separation

Research on gas storage and separation has received more attention since the discovery of MOF. The mechanism of gas adsorption separation is based on the shape or size exclusion of the pores to prevent certain gases from entering the pores of the adsorbent while allowing the target gas to enter and subsequently adsorb. This process is also known as molecular sieving effect [49]. Besides that, the nature of the guest-surface interaction is also important for selective adsorption. For example, the MOF namely $Zn_2(ndc)_2(dpni)$ where dpni and ndc are 2,6-naphthalenedicarboxylate and N,N-di-(4-pyridyl)-1,4,5,8-naphthalene tetracarboxydiimide respectively, is able to adsorb CO_2 over CH_4 as CO_2 exhibits large quadrupole moment [50]. A greater amount of gas can be adsorbed via increasing the surface area of MOF which can be done by

expanding the length of the organic linker, while selective gas can be adsorbed by designing the geometry and shapes of the pores [29]. The MOF compound namely PCN-14 which has the chemical formula of $\text{Cu}_2(5,5'-(9,10\text{-anthracenediyl)-diisophthalate})$, is found to have nanosized cage that can accommodate methane [51]. Study shows that high surface area is not the main factor for high methane storage as PCN-14 has a Langmuir surface area of only 2176 m^2/g , albeit PCN-14 was found to have an absolute uptake capacity of 253 cm^3/g at 290 K and 35 bar which is higher compared to other MOF [51]. The use of PCN-14 for methane storage is potentially less explosive compared to the current compressed nature of gas in vehicles (greater than 200 bar) [51]. Thus, the characteristics of MOF such as ordered structures, adjustable chemical functionality, and highly crystalline porosity represents a class of porous material that is feasible for gas storage and separation [4].

2.6.2 Catalytic reaction

MOF which is mainly composed of metal nodes and linked with organic ligand, allows great chemical and structural diversity [9], [52]. Thus, as the auxiliary compounds were removed from the metal sites, the free metal sites can act as the active sites for catalytic application. The high surface area and uniform pores sizes of the compound also provides high density, uniform non-leaching catalytic centers which are versatile for catalytic reaction [53]. Thus, MOF has been a heterogeneous catalysis candidate to complement other porous solids such as zeolites and mesoporous metal oxides [54]. Although MOF undergoes structural decomposition above temperature 300 °C, liquid-phase reactions can be carried out at a temperature below 200 °C. Therefore, high thermal stability is not a mandatory requirement for a good liquid-phase catalyst. FeBTC has been reported to have great catalytic properties for organic synthesis [55].

Besides that, FeBTC also shows photocatalytic properties for the degradation of dyes as it is a Lewis acid solid [56]. Interestingly, Zhang *et al.* [57] have also reported the selective catalytic reduction of NO_x with the use of bimetallic MOF, MIL-100 (Fe-Mn).

2.6.3 Liquid phase adsorption

Various reports have shown that it is possible to use MOF as an adsorbent to remove hazardous pollutants from water [58], [59]. The large porosity of MOF has played an important role in the adsorptive removal process. The textural characteristic such as pore size and pore geometry are the controlling parameter of the adsorption process [60]. Hydrogen bonding interaction, electrostatic interaction, π - π interaction and acid-base interaction are the mechanism that controls the adsorption process when the size of the target pollutant molecule is greater or similar to the pore size [60]. As the size of the pollutant molecule is greater or similar to the pore size on the compound, size exclusion effect occurs and the pollutant will only adsorbed on the surface of the adsorbent [61].

The most common phenomenon during adsorptive removal from water is electrostatic interaction. Depending on the pH point of zero charge (pH_{pzc}), the surface charge of the MOF changes according to the pH of the environment. When pH_{pzc} of MOF is greater than pH of water, MOF is negatively charge and vice versa. Therefore, the charged MOF can interact with the oppositely charged adsorbates, thus attracting the adsorbate to be adsorbed on the surface of MOF [62].

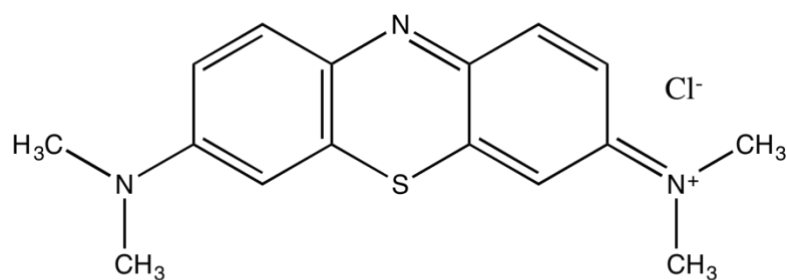
The tuneable pore size MOF also plays an important role in the adsorption and selection of target adsorbate [63]. Adsorbate molecules that are smaller than the pores are allowed to diffuse into the pores, while larger molecules are not adsorbed [64]. MOF also display a faster rate to adsorb smaller and flexible molecules. The MOF pore size

can also be controlled by adding a structure directing-agent such as cationic surfactant cetyltrimethylammonium bromide (CTAB) during synthesis to produce a hierarchically mesostructured MOF. Huang et al. [65] show micro-structured MIL-101 has negligible adsorption towards MB dye, albeit addition of CTAB during synthesis yielded a mesostructured MIL-101 which has great adsorption towards MB dye.

2.6.4 Methylene blue dye adsorption

The use of dye has increased since the surge of human population and economic development [66]. Textile industries are one of the major consumer of high quality dye. However, statistics show that more than 150 million m³ of coloured effluent is discharged as waste water every year and causes severe pollution to the environment [61]. Thus, the textile industry has been recognised as the major source for water pollution. The presence of dye in wastewater will reduce the amount of sunlight for aquatic plants and affect underwater ecosystem [67]. Besides that, the consumption of the polluted water will also cause carcinogenic and mutagenic effect to human bodies. As most of the dye are resistant to degradation, the use of porous material for adsorption is considered as the promising alternative for the removal of dye from wastewater [46], [68].

Figure 2.7 shows the chemical structure of MB dye. MB dye is a widely used cationic dye [69]. MB dye can cause permanent injury to human and animals when contact with the eye. Inhalation of MB can give rise to short periods of breathing difficulty, while ingestion through mouth will cause a burning sensation and may cause nausea, vomiting, profuse sweating, mental confusion, painful micturition and methemoglobinemia [70]. Therefore, the treatment of effluent containing such dye must be properly conducted to reduce its impacts on ecosystem and human health.



Methylene blue

Figure 2.7 Chemical structure of MB.

Various materials such as activated carbon [71], kaolin [70], zeolite [72], lignite [73] and chitosan [74] have been employed to study the adsorption performance against MB dye. Since the discovery of MOF, scientists have been giving more attention on utilising MOF for the adsorption of dye [8], [60], [75]. The tuneable pore size, structure and different metal center are features used to design better adsorbents with higher adsorption capacity and higher adsorption rate for the application [45], [76].

Table 2.1 shows the various preparation methods of CuBTC and its effect on MB dye adsorption. CuBTC can be composed of a second material to enhance the adsorption capacity. Wang *et al.* [77] demonstrated the incorporation of CuBTC on to acrylonitrile butadiene styrene (ABS) which act as the filament of three-dimensional printing material. The three-dimensional printed product shows greater adsorption capacity (64.30 mg/g) of MB compared to naked CuBTC (15.28 mg/g) [77]. Rizwan Azhar *et al.* [78] attempted to produce binary MOF by mixing two MOF precursor solution to enhance the performance of CuBTC. The binary product was a combination of UiO-66 ($Zr_6O_4(OH)_4(OOC-C_6H_4-COO)_6$) and CuBTC. The CuBTC/UiO-66 samples shows almost 3 times adsorption capacity, q_e (41.9 mg/g) of the raw CuBTC. In a separate study, addition of graphite oxide (GO) powder into the CuBTC precursor solution produced a mixture compound that can achieve q_e of 183.49 mg/g [79]. Thus,

addition of a second material to CuBTC can greatly enhance the adsorption performance.

In general, the solvothermal synthesis method is one of the most popular methods used to prepare CuBTC [8], [80]. Hu *et al.* [80] proved that increasing duration and number of times of solvent exchange will also enhance the adsorption capacity of CuBTC. However, it commonly employs huge amounts of dimethylformamide (DMF) and ethanol (EtOH) during the synthesis procedure [78], [80]. As such, a less energy consumption method that utilizes only H₂O as solvent is desired. However, the adsorption capacity of the product should be greater or equal compared to CuBTC prepared via solvothermal synthesis.

Table 2.1 Adsorption capacity of modified and un-modified CuBTC against MB dye.

Sample	Synthesis method	Solvent	Modification	q _e (mg/g) ^a	Reference
CuBTC	Solvothermal	EtOH/DMF	-	15.28	[8]
CuBTC	Solvothermal	EtOH/DMF /H ₂ O	3 times solvent exchange with DMF and EtOH every 24 h	143.27	[80]
CuBTC/ABS	Room temperature	EtOH/H ₂ O	Composite with ABS	64.30	[77]
HKUST-1 /UiO-66	Solvothermal	EtOH/DMF	Composite with UiO-66 MOF	41.9	[78]
HKUST-1 /GO	Solvothermal	EtOH/H ₂ O	Composite with GO	183.49	[79]

^aAdsorption capacity against MB

2.7 Polymer

Firstly, the fundamental building unit of a polymer is called monomer. The word monomer is a derivative of a Greek term *mono*, which means “one” and the term *meros*, which means “part” [81]. A monomer is usually an individual network of the atom or discrete molecules which act as the elementary repeating units in a macromolecular chain [81], [82]. These monomers are linked chemically during a process called polymerization, which usually involve the sharing of electrons to form the polymer. The polymer is used in many applications, such as drug delivery, coating, adhesive, foams, packaging, textile, electronic devices and optical devices [82].

2.7.1 Synthetic polymer

Synthetic polymers namely plastics are manmade polymers which are made from extraction of oil, coal and natural gas [83]. The great durability and stability of plastic allows this material to withstand many environmental influences including microbial attack. Approximately 30% of worldwide plastic are used for packaging application as they have replaced paper and other cellulose-based products because of their better strength and lightness. Plastic is resistance to water and most water-borne microorganisms. Thus, makes it the best material for packaging [83]. Figure 2.8 shows the chemical structure of some of the widely used plastics in packaging, namely polyethylene (PE), polyvinyl chloride (PVC), polypropylene (PP), polystyrene (PS), polyethylene terephthalate (PET) and polyurethane (PU) [83]. Since the increase in demand and production of plastics during the last decades, the littering and waste management of these bulk xenobiotic materials has caused serious problem to the environment [84]. Therefore, about twenty years ago scientists have started to design

polymers that are biodegradable while maintaining their favourable properties. Thus, research of biodegradable polymers have gained more attention over the years [84].

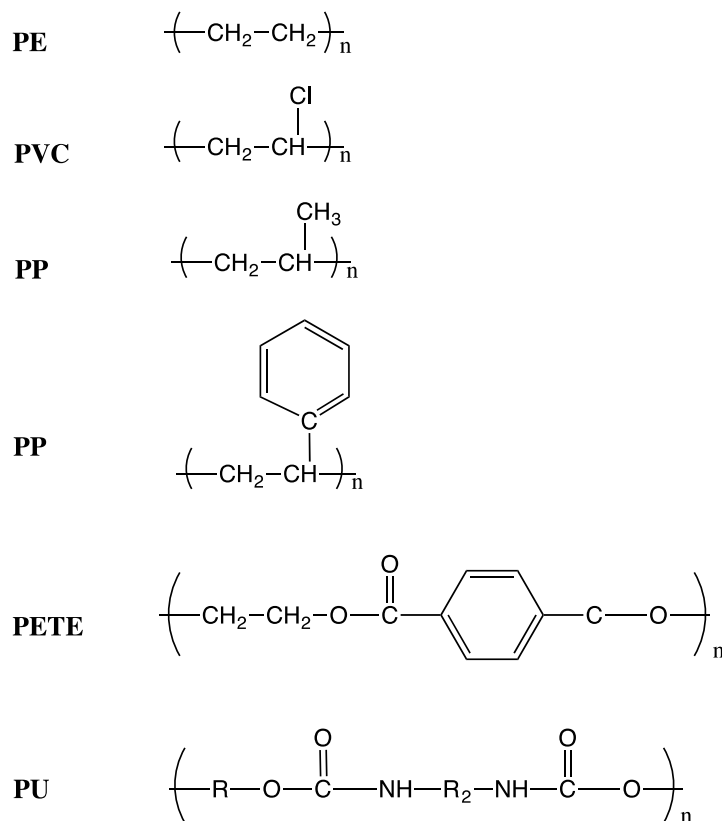
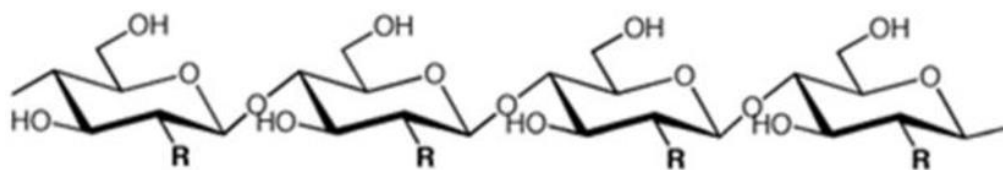


Figure 2.8 Chemical structure of polymers.

2.7.2 Natural polymer

Polymer are classified based on their origin, solid state, thermal response, mode of formation, line structure and biodegradability [82]. Polysaccharides, proteins, polypeptides, and polyesters are natural polymers which originate from a renewable resource and can be obtained from plant and animal sources. Polysaccharides (Figure 2.9) and proteins are the best candidates to replace synthetic polymers among natural polymers due to their abundance in the environment [85]. Therefore, materials such as

rubber, cellulose, and protein has widely been used in many applications before the presence of synthetic polymer [82], [83].



Cellulose : R = OH

Chitin : R = NHC₂H₅

Chitosan : R = NH₂

Figure 2.9 Chemical structure of linear polysaccharides such as cellulose, chitin and chitosan.

2.7.2(a) Polyhydroxyalkanoates (PHA)

Biodegradable polyesters such as polyhydroxyalkanoates (PHA), polylactides and polysaccharides have been successfully developed over the last few years. PHA is produced from the fermentation process of PHA producing microorganism. Therefore, PHA is biodegradable, biocompatible and environmentally friendly [83]. Among the PHA family, polyhydroxybutyrate (PHB) (Figure 2.10) is one of the most studied material [86]. PHB is a highly crystalline polymer which can be synthesized by a variety of Gram-positive and Gram-negative bacteria [87]. High surface area electrospun PHB membranes exhibited excellent adsorption against Malachite green. The study also shows that the immobilization of nano-sized titanium dioxide onto PHB was able to degrad Malachite green dye [87]. No significant loss of TiO₂ from the PHB was found even after ten times application. Photocatalyst immobilized PHB was found to retain its biodegradability. PHB is able to be fully degrad in two months when buried 20 cm under soil and above the mangrove sediment [86], [88]. Thus, the production of an

environmental friendly catalyst is feasible with the use of PHB as the support of the catalyst [89]. This further suggests the possibility of producing an environmental friendly adsorbent with the use of PHB.

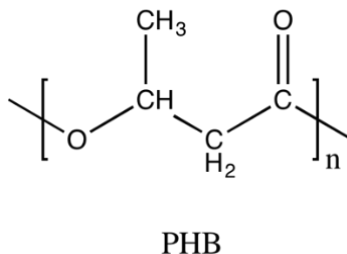


Figure 2.10 Molecular structure of polyhydroxybutyrate.

2.8 Immobilization of MOF

2.8.1 Mixed-matrix membrane

Mixed matrix membrane (MMM) is a type of membrane formed by incorporating fillers in polymer matrix [90]. Polymer is an irreplaceable material for preparation of mixed-matrix membrane due to their low cost, rich category and high processing ability [91]. Polymer membrane has low chemical stability and selectivity, albeit addition of a filler such as zeolite and MOF to form MMM (Figure 2.11), can enhance the characteristic and efficiency of the membrane to suit specific application [92]–[94]. MMM can easily be fabricated by mixing MOF in the polymer solution homogeneously via sonication. The solution is poured into a casting medium and upon removal of solvent, the membrane is formed [94]. By this approach, a polycrystalline MOF membrane that is easily processable [94]. However, MMM is generally reported in gas separation application. MMM demonstrated higher selectivity for ethylene/ethane and H₂/CH₄ gases compared to pure polymer membrane [95], [96].